Full-length article

Knee alignment correction by high tibial osteotomy reduces symptoms and synovial inflammation in knee osteoarthritis accompanied by macrophage phenotypic change from M1 to M2

Running title: HTO changes macrophage polarization in knee OA

Authors

Shigeo Yoshida, MD[1], Kohei Nishitani, MD, PhD[1], Hiroyuki Yoshitomi, MD, PhD[2], Shinichi Kuriyama, MD, PhD[1], Shinichiro Nakamura, MD, PhD[1], Takayuki Fujii, MD, PhD[1,3], Motoo Saito, MD, PhD[1], Yu Kobori, MD[1], Akinori Murakami, MD[1,2], Koichi Murata, MD, PhD[1,3], Hiromu Ito, MD, PhD[1,4], Hideki Ueno, MD, PhD[2,5], Shuichi Matsuda, MD, PhD[1]

Affiliations

[1] Department of Orthopaedic Surgery, Graduate School of Medicine, Kyoto University, Kyoto, Japan

[2] Department of Immunology, Graduate School of Medicine, Kyoto University, Kyoto, Japan

[3] Department of Advanced Medicine for Rheumatic Diseases, Graduate School of Medicine, Kyoto University, Kyoto, Japan

[4] Department of Orthopedic Surgery, Kurashiki Central Hospital, Kurashiki, Japan

[5] Principal investigator, ASHBi Institute for the Advanced Study of Human Biology, Kyoto University, Kyoto, Japan

Corresponding author

Kohei Nishitani MD, PhD

Affiliation: Department of Orthopaedic Surgery, Graduate School of Medicine, Kyoto University

Address: 54 Shogoin-Kawahara-cho, Sakyo-ku, Kyoto 606-8507, Japan

Phone: +81-75-751-3366 Email: nkohei@kuhp.kyoto-u.ac.jp

Funding

This work was supported by Grant-in-Aid for Scientific Research (Grant Number: 18H02927, 20K09408, 21H03053).

Competing Interests

SK received a research grant from Olympus-Terumo Biomaterials Corp. outside of this study.

Abstract

Objective: This study aimed to determine whether alignment correction by high tibial osteotomy (HTO) can change the biological intra-articular microenvironment of osteoarthritic (OA) knees.

Methods: Synovial tissues (STs) and fluids (SFs) were collected from the OA knees of 31 patients during initial HTO and plate removal surgeries. Changes in gene expression in STs were investigated by microarray and real-time polymerase chain reaction (PCR). STs were also evaluated histologically using synovitis scores and immunofluorescence staining to determine macrophage polarity. Cytokines and chemokines in SFs were analyzed by enzyme-linked immunosorbent assays. The mechanism of macrophage polarization was investigated in human peripheral blood mononuclear cells derived macrophages and fibroblast like synoviocytes (FLSs) stimulated with cartilage fragments. We also evaluated Spearman correlations between knee injury and osteoarthritis outcome scores (KOOS) and macrophage-related gene expression.

Results: The microarray results indicated downregulated inflammatory genes and pathways. Real-time PCR determined that genes expressing pro-inflammatory *IL1B* and *IL6*, and M2 macrophage-related *IL1RA*, *IL10*, *CCL18*, and *CD206* genes were respectively downregulated and upregulated. Histological findings revealed attenuated synovitis scores and a shift from M1 to M2 macrophages. Interleukin-1β concentrations in SF decreased after HTO. Cartilage

fragments were responsible for M1 macrophage polarization and pro-inflammatory genes and proteins expression in macrophage, whereas cartilage fragments upregulated only IL-6 protein in FLSs. Postoperative KOOS positively correlated with the expression of the M2-related genes *CCL18* and *CD206*.

Conclusion: Correction of lower-limb alignment with HTO attenuated synovial inflammation and changed macrophage polarization from M1 to M2, suggesting an improved intra-articular environment of knee OA.

Introduction

Osteoarthritis (OA) is the leading cause of disability worldwide. In particular, knee OA causes pain and distress in >20% of elderly patients and limits their quality of life (1). Disease-modifying drugs for knee OA are unknown, and arthroplasty is eventually performed on end-stage patients to alleviate severe symptoms. Knee OA has long been considered a “wear and tear” disease due to mechanical loading that leads to loss of cartilage (2). OA is not presently regarded as a wear and tear condition but rather a multifactorial disease that affects whole joint tissues and is characterized by progressive degeneration of the articular cartilage, subchondral bone remodeling, osteophyte formation, and synovial inflammation (3). Accumulating evidence suggests that synovial inflammation is associated with knee symptoms and progressive OA (4).

Malalignment is a major risk factor for knee OA. A large knee adduction moment in varus knee alignment increases pressure loading on the cartilage, which causes the breakdown of the cartilage matrix and subsequent joint space narrowing (5,6). The mechanism of cartilage breakdown is complex and is not simply wear and tear. Micro cartilage fragments enhance the production of pro-inflammatory cytokines and matrix degradation enzymes, which further accelerate cartilage destruction (7). The progression of OA is thought to be irreversible, but correction of malalignment by knee osteotomies, such as high tibial (HTO) and distal femoral osteotomy, can relieve symptoms and functions while preserving OA joints (8). Although

biomechanical findings have shown that HTO decreases medial compartment loading (9-14), whether inflammation and the production of matrix degradation enzymes in the biological microenvironment are altered by optimizing knee alignment after correction remains unclear. Biological and biomechanical improvements would be ideal for achieving the “remission” of progressive knee OA.

Synovial inflammation has been reported as the precursor of OA onset (15). Several studies have reported that synovial macrophages are positively correlated with OA progression and disease severity; thus, synovial macrophages play an important role in synovitis of OA (16,17). Macrophages can be broadly classified into classically activated M1 macrophages and alternatively activated M2 macrophages in response to their microenvironmental stimuli (18). In the murine model, synovial macrophage M1 polarization accelerates the experimental collagenase-induced OA progression, whereas M2 polarization significantly alleviates OA development (19).

The role of macrophages in knee OA, especially in realignment surgery, is poorly understood. Information about biomarkers and micro-RNA (miRNAs) in synovial fluid (SF) and blood is also scant (20,21), and the environment of the knee joint after alignment correction has not been comprehensively investigated as far as we can ascertain. Therefore, we investigated changes in the biological microenvironment of the knee joint after HTO. We postulated that correcting the extra-articular alignment by HTO would result in decreased intra-articular

inflammatory cytokine expression and catabolic factors, and synovitis.

Materials and Methods

Study participants

This study was approved by the Kyoto University Graduate School and Faculty of Medicine, Ethics Committee (R1529) and was performed per the principles of the Declaration of Helsinki. All patients provided written informed consent to participate. Consecutive patients who underwent medial open-wedge HTO between June 2018 and May 2020 for isolated medial compartment knee OA with varus malalignment were prospectively included. The exclusion criteria comprised patients with inflammatory arthritis, coexisting osteonecrosis, and a history of surgery on the ipsilateral knee other than surgery on the meniscus, who underwent a revision or an additional surgery after initial HTO before plate removal, and whose plate was not removed.

Clinical and radiological evaluation

We preoperatively and postoperatively (at the time of plate removal) determined knee injury and osteoarthritis outcome scores (KOOS) and evaluated standing full-length anteroposterior radiographs of the lower limbs. Knee OA was graded using the Kellgren–Lawrence classification (22). Knee alignment was assessed by measuring the hip–knee–ankle (HKA) angle and weight-bearing line (WBL) ratio (<50% indicates varus alignment) (23). The HKA

angle is determined as the angle between the line connecting the hip and knee center and the line connecting the knee and ankle center. The WBL was drawn from the center of the femoral head to the center of the superior articular surface of the talus. The WBL ratio was defined as the perpendicular distance from the WBL to the medial edge of the tibial plateau divided by the width of the tibial plateau. Medial and lateral joint space width was measured to identify whether radiological improvement was achieved.

Surgical procedure

Patients were treated by HTO as previously described, with a target WBL ratio of 62.5% (24). Two Osferion60 β-tricalcium phosphate wedge spacers (Olympus-Terumo Biomaterials, Tokyo, Japan) were inserted into the gap, and the osteotomy was fixed with TomoFix™ Medial High Tibial Plate (DePuy Synthes, Oberdorf, Switzerland). Full weight-bearing was allowed from 4 weeks after surgery. Synovial tissue (ST) and SF samples were collected at the initial HTO and before removing the plates at about one year after HTO when bone healing was confirmed. SF was aspirated without lavage using the superior-lateral suprapatellar approach. Thereafter, cartilage status in the medial femoral condyle (MFC) was evaluated by arthroscopy using the International Cartilage Repair Society (ICRS) classification (25), and ST samples were obtained from the suprapatellar pouch. The weighted kappa coefficient for the ICRS classification by two investigators (SY and YK) was 0.85.

Isolation of RNA

Total RNA from STs was extracted from fresh samples using a TRIzol reagent (Thermo Fisher Scientific Inc., Waltham, MA, USA) and purified using RNeasy Mini Kits (Qiagen, Hilden, Germany) according to the manufacturer's protocol.

Microarray analysis

Total RNA from three pre- and postoperative pairs from the first 5 HTO patients passing optimal quality control was analyzed using human Clariom™ S Assay microarrays (Thermo Fisher Scientific Inc.), and genes of interest were analyzed using Affymetrix Transcriptome Analysis Console v. 4.0.2. We used the DAVID database (https://david.ncifcrf.gov/) for annotation visualization and integrated discovery. Expressed genes with $P < 0.05$ and ±2-fold changes obtained by performing paired analysis were considered significant. Gene Ontology (GO) and Kyoto Encyclopedia of Genes and Genomes (KEGG) pathways were analyzed using the adjustment of false discovery rate (FDR) values. Cell proportions were determined by deconvolution analysis using MuSiC (26) based on single-cell sequencing data (27).

Real-time reverse transcription–polymerase chain reaction (qRT-PCR)

First-strand complementary DNA was reverse-transcribed from purified RNA using ReverTra Ace® qPCR RT Master Mix (TOYOBO, Osaka, Japan) as described by the manufacturer, then qRT-PCR proceeded using SYBR Green Real-time PCR Master Mix (TOYOBO) on an ABI Step One Plus RT-PCR System (Thermo Fisher Scientific Inc.). Based on the leading microarray signals, genes of interest were selected, and qRT-PCR was performed on all 31

patients, including 3 patients for whom microarray analyses were performed. The relative expression of target genes was normalized to the expression of glyceraldehyde-3-phosphate dehydrogenase (*GAPDH*) and calculated by the $2^{\Delta\Delta CT}$ method. All assays were performed in duplicate. Supplementary Table 1 shows the PCR primers.

Histological analysis and immunofluorescence

Synovium samples were immediately embedded in the Tissue-Tek OCT compound (Sakura Finetek Japan, Tokyo, Japan), frozen by liquid nitrogen, and stored at −80 °C until sectioning. Frozen sections were cut into 12-µm sections, fixed in 4% paraformaldehyde (PFA) for 15 min, and were histologically stained with hematoxylin and eosin stain to evaluate the synovial activation using Krenn synovitis scores (28). Three components of synovitis (lining layer hyperplasia, activation of stroma cells, and inflammatory infiltrate) were each scored from 0–3 and summed to a total score ranging from 0–9, with scores of 1–4 indicating low-grade synovitis and scores of 5–9 indicating high-grade synovitis. The weighted kappa coefficient for this scoring by two investigators (SY and YK) was 0.77. For immunofluorescence, sections were fixed in 4% PFA for 15 min and immersed in HistoVT One (Nacalai Tesque, Kyoto, Japan) for 20 min at 60 °C to unmask the antigen. Sections were left to cool for 15 min before being washed twice in phosphate-buffered saline (PBS). The sections were blocked using 10% goat serum at room temperature for 1 h and were stained with primary immunofluorescent antibodies to detect the macrophage marker CD68 (ab955) or CD11b (ab34216), the M1-like

macrophage marker CD80 diluted at 1:250 (ab134120), the M2-like macrophage marker CD206 diluted at 1:500 (ab64693), and the tissue-resident macrophage marker lymphatic vessel endothelial hyaluronan receptor 1 (LYVE1) diluted at 1:250 (ab33682; all from Abcam, Cambridge, UK) (29), followed by Alexa Fluor 488 goat anti-mouse IgG secondary antibodies diluted at 1:250 (A-11029), Alexa Fluor 555 goat anti-rabbit IgG diluted at 1:250 (A-21429) in Can Get Signal® immunostain Solution B (TOYOBO) at room temperature for 1 h. After incubation, stained sections were washed three times in PBS and mounted with Prolong® Gold Antifade Reagent with 4′,6-diamidino-2-phenylindole (all from Thermo Fisher Scientific Inc.). Fluorescence images were analyzed using a BZ-X710 microscope (Keyence, Osaka, Japan).

Synovial fluid analysis

The SF samples were centrifuged, and the supernatants were stored at –80 °C. The cytokine profiles of the interleukin (IL)-1RA, IL-6, IL-10, IL-13, CCL3 (MIP-1α), tumor necrosis factor (TNF)-α, and the interferon (IFN)-γ in SF were analyzed using Pro-Human Cytokine Multiplex Assays (Bio-Rad Laboratories Inc., Hercules, CA, USA) and Quantikine ELISA Kits (R&D Systems, Minneapolis, MN, USA) for IL-1β. All assays were performed in duplicate. The number of cartilage fragments in SF was analyzed using Countess (Thermo Fisher Scientific Inc.) without centrifugation in additional SF samples collected between July and December 2021 from seven patients during HTO and seven at the time of plate removal after HTO.

Primary macrophage and fibroblast-like synoviocytes (FLS) stimulation *in vitro*

Peripheral blood mononuclear cells (PBMCs) from total 6 healthy donors were obtained by density gradient centrifugation with Lymphocyte Separation Solution® (Nacalai Tesque) (30,31). CD14+ monocytes were isolated using CD14 magnetic microbeads (Miltenyi Biotec, Bergisch Gladbach, Germany) according to the manufacturer's protocol. CD14+ monocytes were cultured at a density of 0.5×10^6 cells/mL with 50 ng/mL macrophage colony-stimulating factor (M-CSF) (Pepro Tech, Cranbury, NJ, USA) for the generation of macrophages. On day 3, the M-CSF supplemented medium was refreshed. On day 6, cells were washed and used for functional assays. Cells were cultured in the RPMI 1640 medium (Gibco; Thermo Fisher Scientific, Waltham, MA, USA), supplemented with 10% fetal bovine serum (FBS; MP Biomedicals, Santa Ana, CA, USA), 2 mM glutamine, 100 U/mL penicillin, and 100 μg/mL streptomycin (Gibco; Thermo Fisher Scientific) at 37 °C with 5% CO_2. To confirm the presence of differentiated macrophages, immunofluorescence staining for CD68 (Abcam) was performed as previously described. We evaluated the effects of humoral factors in SF on macrophages stimulated using a medium containing 50% SF obtained during HTO or plate removal, then RNA was extracted. FLS were cultured using human STs obtained from total knee arthroplasty (TKA) in 5 patients with OA as previously reported (32). Briefly, STs were minced and digested with 2 mg/mL collagenase (Wako, Osaka, Japan) in Dulbecco's Modified Eagle's Medium (DMEM; Sigma Aldrich, St. Louis, MO, USA) containing 100 U/mL penicillin and 100 μg/mL streptomycin at 37 °C for 2 h, followed by digestion with 0.05%

trypsin and 0.02% ethylenediaminetetraacetic acid (EDTA) at 37 °C for 30 min. The cells were cultured in DMEM containing 10% FBS (MP Biomedicals) in 100-mm dishes (Iwaki, Tokyo, Japan) at 37 °C in a humidified 5% CO_2 atmosphere. After 3–5 passages, FLSs were plated on 60-mm dishes (Corning, NY, USA) in DMEM containing 10% FBS for assays. Cartilage fragments were prepared from the cartilage tissues of patients with primary OA who underwent TKA. As previously described (33), isolated cartilages were rinsed using ice-cold PBS and then crushed twice at 2000 rpm for 10 s using Medical Beads Shocker (Yasui Kikai, Osaka, Japan) with chamber and ball precooled with liquid nitrogen, then cartilage fragments were filtered by 40 μm porous nylon mesh filters to remove large cartilage fragments. The number and size of cartilage fragments were assessed using Countess (Invitrogen). The cartilage fragments were confirmed to be comparable in size to the cartilage fragments isolated from OA SF (34,35) (Supplementary Figure 1). The cartilage fragments were kept at −80 °C until further use. PBMC derived macrophages and FLSs were cultured with or without cartilage fragments at a ratio of 1:3 (low density) and 1:10 (high density) for 24 h. The macrophages were harvested, and CD80 immunostained with fluorescent antibodies was quantified as fluorescence emission using Image Analyser (KEYENCE). Total RNA was extracted to analyze gene expression with TATA-binding protein (*TBP*) as a housekeeping gene for macrophages and *GAPDH* for FLSs. Enzyme-linked immunosorbent assay was performed to measure the concentration of human IL-1β, IL-6, and TNF-α in culture supernatants using Quantikine ELISA Kits (R&D Systems).

Statistical analysis

The results are presented as the means ± standard deviation for normally distributed data and as medians with interquartile ranges for non-normally distributed data. Clinical data from samples obtained during HTO and plate removal were compared by the Wilcoxon matched-pairs signed-rank tests unless otherwise indicated. The numbers of cartilage fragments were compared by Mann–Whitney U tests. The effects of SF and cartilage fragments on primary macrophages and FLSs *in vitro* were analyzed by paired t-tests and one-way analyses of variance with Tukey post-hoc tests, respectively. Correlations between KOOS and synovial gene expression were determined by Spearman rank correlations. Statistical analyses were performed using GraphPad Prism version 9.1.2 (GraphPad Software, San Diego, CA, USA) or SPSS version 24.0 (IBM, Armonk, NY, USA). Values with $P < 0.05$ were considered statistically significant.

The sample size was calculated using R 3.3.1 (R foundation, Vienna, Austria) with the EZR (Saitama Medical Center, Jichi Medical University, Saitama, Japan) plug-in with power = 0.8 and alpha error = 0.05 based on changes in synovial gene expressions because of drug treatment and changes in protein levels in joint fluid because of surgical intervention (n = 25 and n = 20, respectively) (20,36). A post-hoc power analysis using alpha error = 0.05 for M2-related genes revealed powers of 0.92 and 0.81 in the 31 patients for *CCL18* and *CD206*, respectively.

Results

Characteristics of the patients

A total of 40 consecutive patients were initially included, then five patients with osteonecrosis and three without plate removal due to unrelated reasons to the postoperative course were excluded. One patient with a surgical site infection who needed additional surgery was also excluded. Table 1 shows the demographics and clinical features of the 31 patients who were included in the study. Plates were removed 13.2 ± 2.2 months after HTO. The ICRS classification of MFC improved in 11 (35%) patients after HTO, and deterioration was not evident. Medial joint space width was increased after HTO, and lateral joint space width was maintained.

Microarray analysis

Microarray analysis of the three patients identified 477 differentially expressed genes (DEGs) between the samples obtained during HTO and plate removal. Of these, 252 were upregulated, and 225 were downregulated after plate removal compared with HTO (Figure 1A). Supplementary Table 2 shows each of the top 20 upregulated and downregulated DEGs. The GO results of the DEGs showed that the downregulated genes were mainly associated with inflammatory processes, such as cellular response to tumor necrosis factor, neutrophil chemotaxis, cellular response to IL-1 and chemokine-mediated signaling pathway, inflammatory response, and monocyte chemotaxis (Figure 1B). No upregulation-associated

GO term was observed. The KEGG pathway results showed that the upregulated genes were mainly associated with oxidative phosphorylation (Figure 1C). In contrast, inflammatory-related pathways such as the toll-like receptor signaling pathway, rheumatoid arthritis, TNF signaling pathway, cytokine-cytokine receptor interaction, NF-kappa B signaling pathway, and chemokine signaling pathway were downregulated (Figure 1D). The results of analyzing cell deconvolution in STs using MuSiC showed that the proportion of inflammatory macrophages tended to decrease after plate removal, whereas other cellular components were generally similar between HTO and plate removal (Figure 1E).

Gene expression in synovial tissues

Gene expression was compared between the STs collected during HTO and plate removal (Figure 1F). The gene expression of the catabolic enzymes *ADAMTS4*, *MMP1*, *MMP3*, and *MMP13* did not significantly differ. The expression of the inflammatory cytokines, *IL1B* and *IL6*, was downregulated at the time of plate removal, whereas that of *TNFA* was not. Among macrophage-related chemokines and cytokines, the expression of *CCL3* (M1-macrophage-related) was downregulated, and that of *CCL18*, *IL1RA*, and *IL10* (M2-macrophage-related) were upregulated at the time of plate removal. The expression of a surface marker of M2-macrophages *CD206* was upregulated, whereas that of the M1-macrophage markers *CD80* was not significantly altered.

Histological findings

Many hyperplastic cells lined the synovium, and the inflammatory cell infiltration was abundant in HTO (Figure 2A). In contrast, diminished inflammation at the time of plate removal was confirmed by reduced synovitis scores (P <0.001) (Figure 2B). The proportions of CD80 and CD206 positive macrophages in the synovium were respectively decreased and increased one year after HTO (Figure 2C–F). The polarity of macrophages was tested using CD11b as an alternative macrophage marker to CD68, and consistent trends were observed (Supplementary Figure 2A-D). The proportions or location of LYVE1-positive macrophages as tissue-resident macrophages in the synovium were not changed one year after HTO (Supplementary Figure 2E and F).

Synovial fluid findings

Supplementary Table 3 shows the cytokine profiles of preoperative and postoperative SF. The median concentration of IL-1β was reduced from to 0.62 pg/mL (interquartile range: 0.22-1.26 pg/mL) to 0.22 pg/mL (interquartile range: not detectable -0.87 pg/mL) after HTO (P = 0.03), whereas the levels of IL-6, TNF-α, CCL3, IFN-γ, IL-1RA, IL-10, and IL-13 did not change.

Stimulation of macrophages and FLSs *in vitro*

The differentiation of human primary macrophages was confirmed by immunofluorescence staining (Supplementary Figure 3). Stimulating macrophages with humoral factors of SF at

HTO changes macrophage polarization in knee OA

HTO and plate removal did not affect the transcription of pro-inflammatory cytokines or macrophage markers (Supplementary Figure 4). We then investigated the effects of cartilage fragments on macrophages and FLSs. Cartilage fragments were less in the SF at plate removal than during HTO (Supplementary Figure 5). The stimulation of macrophages with a high density of cartilage fragments increased the mean signal intensity of CD80 in the macrophage cytoplasm (Figure 3A and B) and upregulated the pro-inflammatory cytokines (*IL1B* and *IL6*) and *CD80* (Figure 3C) and significantly increased concentrations of IL-1β, IL-6, and TNF-α (Figure 3D). In contrast, the stimulation of FLSs with cartilage fragments did not affect the transcription of pro-inflammatory cytokines (Figure 3E) and increased only IL-6 protein levels (Figure 3F).

Association with clinical findings

The gene expression of M1-associated *CD80* in ST correlated negatively with postoperative (plate removal) and delta (postoperative minus preoperative) KOOS scores, whereas that of M2-associated *CD206* and *CCL18* correlated positively with postoperative KOOS scores (Figure 4).

Discussion

We showed that synovial inflammation in the OA joint might be reversed by correcting knee alignment. The expression of pro-inflammatory cytokines and synovitis was partially

suppressed in STs, and the polarity of synovial macrophages became M2-dominant. Cartilage fragments rather play a more critical role than humoral factors in macrophage polarization. However, catabolic enzymes were not reduced, which was contrary to our hypothesis.

Surgical HTO reduces symptoms and prevents disease progression in younger and active elderly patients by changing the alignment of the lower limb from varus to valgus (37). Biomechanical studies revealed decreased medial compartment loading after HTO (9-14). However, little is known about the effects of HTO on the intra-articular microenvironment. The miR-30c-5p, which regulates macrophage-mediated inflammation and OA pathogenesis, is increased in SF after HTO and correlates with postoperative pain relief (21). Concentrations of IL-6, IL-8, MMP-2, MMP-3, MMP-13, VEGF, and COMP are significantly decreased in SF after HTO (20). However, we found that only IL-1β significantly decreased in SF. These contradictory findings might be due to differences in patient background, disease severity, and the timing of plate removal.

Synovitis is prevalent in patients with OA, and the synovium of OA produces pro-inflammatory cytokines, resulting in low-grade inflammation, but little is known about whether inflammation is reversible (4,38). Our transcriptional and histological findings of improvement of synovial inflammation may indicate that inflammation was reversible. Synovial macrophages are associated with OA progression (16,17). Macrophages are broadly classified as having classically and alternatively activated M1 and M2 phenotypes, respectively (18). Pro-

inflammatory M1 macrophages activated by IFN-γ, lipopolysaccharide, and TNF-α secrete abundant pro-inflammatory cytokines and mediators such as TNF-α, IL -1β, IL-6, and IL-12 (39). Wound-healing M2 macrophages stimulated by IL-4 or IL-13 produce anti-inflammatory cytokines such as IL-10, IL-1RA, and transforming growth factor-β (40). The role of polarized macrophages in the pathogenesis and progression of OA has been highlighted. The ratio of M1 to M2 macrophages is clearly higher in knee OA compared with controls (41). Furthermore, M1, but not M2, macrophages accumulate in human and mouse knee OA synovium, and synovial M1 macrophages exacerbate experimental collagenase-induced OA, whereas M2 macrophages attenuate OA development (42). We found that preoperative synovial macrophages were polarized to the M1 phenotype, whereas they changed to the M2 phenotype upon alignment correction by HTO. The polarization of M2 macrophages might play an anti-inflammatory role in knee OA, possibly contributing to articular cartilage repair.

One explanation for the altered macrophage polarization could be a change in cartilage fragment production. Histological findings of human OA tissues have shown that cartilage fragments in the synovium elicit an inflammatory response (43,44). Cartilage fragments trigger macrophage inflammatory responses *in vitro* that enhance catabolic factors in chondrocytes (33). In the present study, not humoral factors in SF but cartilage fragments affected macrophage polarization. Cartilage fragments also acted on FLS to produce IL-6. A possible mechanism of the effect of HTO is that load bearing shifts from damaged medial cartilage to

less-degenerated lateral cartilage, which decreases the production of cartilage fragments, resulting in the decreased gene expression of pro-inflammatory cytokines in synovial cells, including fibroblast and macrophage, accompanied with macrophage polarization to the M2 phenotype (Figure 5).

This study has several limitations. The sample was relatively small, and our findings depended on the timing of sample collection during HTO and plate removal. Unlike a previous study with a longer follow-up (20), we did not find attenuated catabolic enzymes. We anticipate that the intra-articular biological environment will be further altered by a longer follow-up. However, postoperative samples could not be collected from the patients multiple times because of ethical restrictions. The sample size for microarray was just three. We planned it for the first five patients; however, due to the strict quality control for microarray, three pre- and postoperative pairs were finally available for microarray. Due to the limited samples, FDR adjustment did not yield significant DEGs; hence, a non-adjusted *P* value was used. Thus, the risk of alpha error existed. However, GO and KEGG pathway analyses were performed with FDR adjustment. We postulated the prospect with microarray using a small number of samples, and subsequent analyses were performed for all patients to investigate the hypothesis. We collected synovial samples only from the suprapatellar pouch, although the knee joint has several other synovial sites. A previous magnetic resonance imaging study reported that the most common sites for definite synovitis are posterior to the posterior cruciate ligament (PCL)

in 71.2% of all knees and the suprapatellar region in 59.5% of all knees (45). Sample collection from the posterior of the PCL is challenging, but the suprapatellar pouch can be easily accessed; therefore, the suprapatellar pouch is considered a reasonable sampling site. The effects of different sampling sites were minimized by standardizing the sampling location to the suprapatellar pouch, and the deconvolution results confirmed that the cell distribution was similar between the two sampling times. Although we showed changes in the polarization of macrophages to the M2 phenotype, this did not provide enough evidence that macrophages mainly regulated the synovial inflammatory environment and the tissue responses observed post HTO. Further study is needed to elucidate the precise mechanism of cellular response after alignment changes in synovial tissues. Finally, to evaluate the healing of the cartilage directly, sampling the cartilage at two time points was ideal. However, to protect the cartilage, it was clinically and ethically difficult to harvest the cartilage from the patients.

To conclude, we showed that mechanical realignment alters the biological microenvironment of the knee joint. Surgical HTO is a joint preservation procedure that improves mechanical loading that changes inflammatory status in the knee joint and alters synovial macrophage polarization to a pro-healing phenotype.

Data availability

The data that support the findings of this study are available from the corresponding author

upon reasonable request. Microarray data for this study have been deposited in the NCBI Gene Expression Omnibus database (GSE220596).

References

1. Hunter DJ, Bierma-Zeinstra S. Osteoarthritis. The Lancet 2019;393:1745-59.
2. Dobson GP, Letson HL, Grant A, McEwen P, Hazratwala K, Wilkinson M, et al. Defining the osteoarthritis patient: back to the future. Osteoarthritis Cartilage 2018;26:1003-7.
3. Loeser RF, Goldring SR, Scanzello CR, Goldring MB. Osteoarthritis: a disease of the joint as an organ. Arthritis Rheum 2012;64:1697-707.
4. Robinson WH, Lepus CM, Wang Q, Raghu H, Mao R, Lindstrom TM, et al. Low-grade inflammation as a key mediator of the pathogenesis of osteoarthritis. Nat Rev Rheumatol 2016;12:580-92.
5. Miyazaki T, Wada M, Kawahara H, Sato M, Baba H, Shimada S. Dynamic load at baseline can predict radiographic disease progression in medial compartment knee osteoarthritis. Ann Rheum Dis 2002;61:617-22.
6. Hurwitz DE, Ryals AB, Case JP, Block JA, Andriacchi TP. The knee adduction moment during gait in subjects with knee osteoarthritis is more closely correlated with static alignment than radiographic disease severity, toe out angle and pain. J Orthop Res 2002;20:101-7.
7. Poole AR, Kobayashi M, Yasuda T, Laverty S, Mwale F, Kojima T, et al. Type II collagen degradation and its regulation in articular cartilage in osteoarthritis. Ann Rheum Dis 2002;61 Suppl 2:ii78-81.
8. Birmingham TB, Giffin JR, Chesworth BM, Bryant DM, Litchfield RB, Willits K, et al. Medial opening wedge high tibial osteotomy: a prospective cohort study of gait, radiographic, and patient-reported outcomes. Arthritis Rheum 2009;61:648-57.
9. Agneskirchner JD, Hurschler C, Wrann CD, Lobenhoffer P. The effects of valgus medial opening wedge high tibial osteotomy on articular cartilage pressure of the knee: a biomechanical study. Arthroscopy 2007;23:852-61.
10. Martay JL, Palmer AJ, Bangerter NK, Clare S, Monk AP, Brown CP, et al. A preliminary modeling investigation into the safe correction zone for high tibial osteotomy. Knee 2018;25:286-95.
11. Nakayama H, Schroter S, Yamamoto C, Iseki T, Kanto R, Kurosaka K, et al. Large correction in opening wedge high tibial osteotomy with resultant joint-line obliquity induces excessive shear stress on the articular cartilage. Knee Surg Sports Traumatol Arthrosc 2018;26:1873-8.
12. Kuriyama S, Watanabe M, Nakamura S, Nishitani K, Sekiguchi K, Tanaka Y, et al. Classical target coronal alignment in high tibial osteotomy demonstrates validity in terms of knee kinematics and kinetics in a computer model. Knee Surg Sports Traumatol Arthrosc 2020;28:1568-78.

13. Lind M, McClelland J, Wittwer JE, Whitehead TS, Feller JA, Webster KE. Gait analysis of walking before and after medial opening wedge high tibial osteotomy. Knee Surg Sports Traumatol Arthrosc 2013;21:74-81.
14. Whatling GM, Biggs PR, Elson DW, Metcalfe A, Wilson C, Holt C. High tibial osteotomy results in improved frontal plane knee moments, gait patterns and patient-reported outcomes. Knee Surg Sports Traumatol Arthrosc 2020;28:2872-82.
15. Atukorala I, Kwoh CK, Guermazi A, Roemer FW, Boudreau RM, Hannon MJ, et al. Synovitis in knee osteoarthritis: a precursor of disease? Ann Rheum Dis 2016;75:390-5.
16. Daghestani HN, Pieper CF, Kraus VB. Soluble macrophage biomarkers indicate inflammatory phenotypes in patients with knee osteoarthritis. Arthritis Rheumatol 2015;67:956-65.
17. Kraus VB, McDaniel G, Huebner JL, Stabler TV, Pieper CF, Shipes SW, et al. Direct in vivo evidence of activated macrophages in human osteoarthritis. Osteoarthritis Cartilage 2016;24:1613-21.
18. Sica A, Mantovani A. Macrophage plasticity and polarization: in vivo veritas. J Clin Invest 2012;122:787-95.
19. Zhang H, Lin C, Zeng C, Wang Z, Wang H, Lu J, et al. Synovial macrophage M1 polarisation exacerbates experimental osteoarthritis partially through R-spondin-2. Ann Rheum Dis 2018;77:1524-34.
20. Kumagai K, Fujimaki H, Yamada S, Nejima S, Matsubara J, Inaba Y. Changes of synovial fluid biomarker levels after opening wedge high tibial osteotomy in patients with knee osteoarthritis. Osteoarthritis Cartilage 2021;29:1020-8.
21. Kwak YH, Kwak DK, Kim NY, Kim YJ, Lim JS, Yoo JH. Significant changes in synovial fluid microRNAs after high tibial osteotomy in medial compartmental knee osteoarthritis: Identification of potential prognostic biomarkers. PLoS One 2020;15:e0227596.
22. Kellgren JH, Lawrence JS. Radiological assessment of osteo-arthrosis. Ann Rheum Dis 1957;16:494-502.
23. Moreland JR, Bassett LW, Hanker GJ. Radiographic analysis of the axial alignment of the lower extremity. J Bone Joint Surg Am 1987;69:745-9.
24. Kuriyama S, Morimoto N, Shimoto T, Takemoto M, Nakamura S, Nishitani K, et al. Clinical efficacy of preoperative 3D planning for reducing surgical errors during open-wedge high tibial osteotomy. J Orthop Res 2019;37:898-907.
25. Brittberg M, Winalski CS. Evaluation of cartilage injuries and repair. J Bone Joint Surg Am 2003;85-A Suppl 2:58-69.
26. Wang X, Park J, Susztak K, Zhang NR, Li M. Bulk tissue cell type deconvolution with multi-subject single-cell expression reference. Nat Commun 2019;10:380.

27. Chou CH, Jain V, Gibson J, Attarian DE, Haraden CA, Yohn CB, et al. Synovial cell cross-talk with cartilage plays a major role in the pathogenesis of osteoarthritis. Sci Rep 2020;10:10868.
28. Krenn V, Morawietz L, Burmester GR, Kinne RW, Mueller-Ladner U, Muller B, et al. Synovitis score: discrimination between chronic low-grade and high-grade synovitis. Histopathology 2006;49:358-64.
29. Mulder K, Patel AA, Kong WT, Piot C, Halitzki E, Dunsmore G, et al. Cross-tissue single-cell landscape of human monocytes and macrophages in health and disease. Immunity 2021;54:1883-900 e5.
30. Murata K, Fang C, Terao C, Giannopoulou EG, Lee YJ, Lee MJ, et al. Hypoxia-Sensitive COMMD1 Integrates Signaling and Cellular Metabolism in Human Macrophages and Suppresses Osteoclastogenesis. Immunity 2017;47:66-79 e5.
31. Wood MJ, Leckenby A, Reynolds G, Spiering R, Pratt AG, Rankin KS, et al. Macrophage proliferation distinguishes 2 subgroups of knee osteoarthritis patients. JCI Insight 2019;4.
32. Tanida S, Yoshitomi H, Nishitani K, Ishikawa M, Kitaori T, Ito H, et al. CCL20 produced in the cytokine network of rheumatoid arthritis recruits CCR6+ mononuclear cells and enhances the production of IL-6. Cytokine 2009;47:112-8.
33. Hamasaki M, Terkawi MA, Onodera T, Homan K, Iwasaki N. A Novel Cartilage Fragments Stimulation Model Revealed that Macrophage Inflammatory Response Causes an Upregulation of Catabolic Factors of Chondrocytes In Vitro. Cartilage 2021;12:354-61.
34. Mendel K, Eliaz N, Benhar I, Hendel D, Halperin N. Magnetic isolation of particles suspended in synovial fluid for diagnostics of natural joint chondropathies. Acta Biomater 2010;6:4430-8.
35. Kuster MS, Podsiadlo P, Stachowiak GW. Shape of wear particles found in human knee joints and their relationship to osteoarthritis. Br J Rheumatol 1998;37:978-84.
36. Kane D, Gogarty M, O'Leary J, Silva I, Bermingham N, Bresnihan B, et al. Reduction of synovial sublining layer inflammation and proinflammatory cytokine expression in psoriatic arthritis treated with methotrexate. Arthritis Rheum 2004;50:3286-95.
37. Amendola A, Bonasia DE. Results of high tibial osteotomy: review of the literature. Int Orthop 2010;34:155-60.
38. Benito MJ, Veale DJ, FitzGerald O, van den Berg WB, Bresnihan B. Synovial tissue inflammation in early and late osteoarthritis. Ann Rheum Dis 2005;64:1263-7.
39. Shapouri-Moghaddam A, Mohammadian S, Vazini H, Taghadosi M, Esmaeili SA, Mardani F, et al. Macrophage plasticity, polarization, and function in health and disease. J Cell Physiol 2018;233:6425-40.
40. Murray PJ, Allen JE, Biswas SK, Fisher EA, Gilroy DW, Goerdt S, et al. Macrophage

activation and polarization: nomenclature and experimental guidelines. Immunity 2014;41:14-20.
41. Liu B, Zhang M, Zhao J, Zheng M, Yang H. Imbalance of M1/M2 macrophages is linked to severity level of knee osteoarthritis. Exp Ther Med 2018;16:5009-14.
42. Zhang H, Lin C, Zeng C, Wang Z, Wang H, Lu J, et al. Synovial macrophage M1 polarisation exacerbates experimental osteoarthritis partially through R-spondin-2. Ann Rheum Dis 2018;77:1524-34.
43. Saito I, Koshino T, Nakashima K, Uesugi M, Saito T. Increased cellular infiltrate in inflammatory synovia of osteoarthritic knees. Osteoarthritis Cartilage 2002;10:156-62.
44. Schedel J, Wenglen C, Distler O, Muller-Ladner U, Scholmerich J, Heinegard D, et al. Differential adherence of osteoarthritis and rheumatoid arthritis synovial fibroblasts to cartilage and bone matrix proteins and its implication for osteoarthritis pathogenesis. Scand J Immunol 2004;60:514-23.
45. Roemer FW, Kassim Javaid M, Guermazi A, Thomas M, Kiran A, Keen R, et al. Anatomical distribution of synovitis in knee osteoarthritis and its association with joint effusion assessed on non-enhanced and contrast-enhanced MRI. Osteoarthritis Cartilage 2010;18:1269-74.

Figure legends

Figure 1. Comparing gene expression profiles in the synovium at initial HTO and plate removal by microarray analysis (n = 3) and real-time reverse transcription–polymerase chain reaction (qRT-PCR) (n = 31). The volcano plot (A) shows the differential expression of 477 genes (red: upregulated and blue: downregulated genes >2-fold change) compared with the synovium at HTO. Representative Gene Ontology (GO) processes of downregulated (B) genes at plate removal. Representative Kyoto Encyclopedia of Genes and Genomes (KEGG) pathway of upregulated (C) and downregulated (D) genes at plate removal. The proportion of cells in the synovium (E) was analyzed by deconvolution analysis with MuSiC using single-cell sequencing data (27). (F) Gene expression (relative to *GAPDH*) of catabolic factors, pro-inflammatory and anti-inflammatory cytokines, chemokines, and macrophage surface markers in synovial tissues at HTO (Pre) and plate removal (Post). qRT-PCR was performed in duplicate and repeated twice. The same patients were connected by lines pre- and post-HTO for all 31 patients, and the three cases used for the microarray were marked in red. Bars indicate medians and interquartile ranges. *: $P < 0.05$, **: $P < 0.01$, and ***: $P < 0.001$ (Wilcoxon matched-pairs signed-rank tests). HTO, high tibial osteotomy; Pre, initial HTO; Post, plate removal

Figure 2. Synovitis scores and macrophage phenotypes at high tibial osteotomy (HTO) (Pre) and plate removal (Post). (A) Representative images of synovial tissue (ST) samples stained

with hematoxylin and eosin showing all three features of the synovitis scoring system. Black scale bars, 200 μm. (B) Synovitis scores. Representative images of double immunofluorescence staining of CD68 and macrophage polarization markers CD80 (C) and CD206 (D) on STs. White scale bars, 50 μm. Percentages of CD80 (E) and CD206 (F) positive *vs.* total macrophages. *P* values were determined by the Wilcoxon matched-pairs signed-rank test. Bars in graphs indicate medians and interquartile ranges.

Figure 3. Stimulation of peripheral blood mononuclear cell (PBMC) derived macrophages and fibroblast-like synoviocytes (FLSs) by cartilage fragments. Representative images (A) of CD80-positive macrophages stimulated with cartilage fragments and stained with immunofluorescence. Scale bars, 20 μm. Mean signal intensity (B) of CD80 in macrophage cytoplasm (n = 5). Gene expression in PBMC derived macrophages (n = 4) (C) and FLSs (n = 5) (E) stimulated with cartilage fragments determined by real-time polymerase chain reaction. The expression of RNA was normalized to those of *TBP* for macrophages and *GAPDH* for FLSs. The concentration of inflammatory cytokines in culture supernatants of macrophages (n = 4) (D) and FLSs (n = 5) (F) stimulated with cartilage fragments. (−) no cartilage fragments; (+) and (++) low- and high-density cartilage fragments, respectively. Bars in graphs indicate the mean and standard deviations. The experiments were performed in duplicate and repeated twice. **P* <0.05, ** *P* <0.01, *** *P* <0.001, by one-way analysis of variance and Tukey post-

hoc tests.

Figure 4. Associations between clinical scores and macrophage-related gene expression. Spearman correlations between gene expression in synovial tissue (ST) and knee injury and osteoarthritis outcome scores (KOOS): total score at plate removal (Post-op) (A) and between gene expression in ST and ΔKOOS: total score between before high tibial osteotomy (HTO) and at plate removal (B). Δ, delta (difference).

Figure 5. Summarized schema of the study. A possible mechanism underlying the beneficial effects of the high tibial osteotomy might be that reducing load-bearing in the damaged medial cartilage decreases cartilage fragment production that results in decreased inflammatory cytokine expression and polarization to M2 macrophages.

Table

Table 1. Demographics showing characteristics of the study population.

n = 31	Pre (at HTO)	Post (at plate removal)	*P*-value
Age, years	61.1 ± 7.5		
Sex, Female (n, %)	19, 61%		
Body mass index, kg/m^2	27.0 ± 4.0		
KL grade 1/2/3/4, (n, %)	3(10)/10(32)/13(42)/5(16)	1(3)/9(29)/15(48)/6(19)	0.18
HKA angle, degree	7.8 ± 4.0 varus	0.9 ± 2.8 valgus	<0.001*
WBL ratio, %	14.9 ± 16.7	53.4 ± 11.4	<0.001*
KOOS, point	60.1 (47.0–69.6)	86.3 (75.6–91.1)	<0.001
ICRS grade 2/3/4, (n, %)	2(6)/15(48)/14(45)	8(26)/14(45)/9(29)	0.001
Medial JSW, mm	2.3 ± 1.7	2.8 ± 1.2	<0.001*
Lateral JSW, mm	6.1 ± 1.8	5.8 ± 1.5	0.07*

HTO, high tibial osteotomy; KL, Kellgren–Lawrence; HKA, hip–knee–ankle; WBL, weight-bearing line; KOOS, Knee injury and Osteoarthritis Outcome Score; ICRS, International Cartilage Repair Society; JSW, joint space width. *P* values were calculated with the Wilcoxon matched-pairs signed-rank test except for * (Paired t-test).

Figure 1

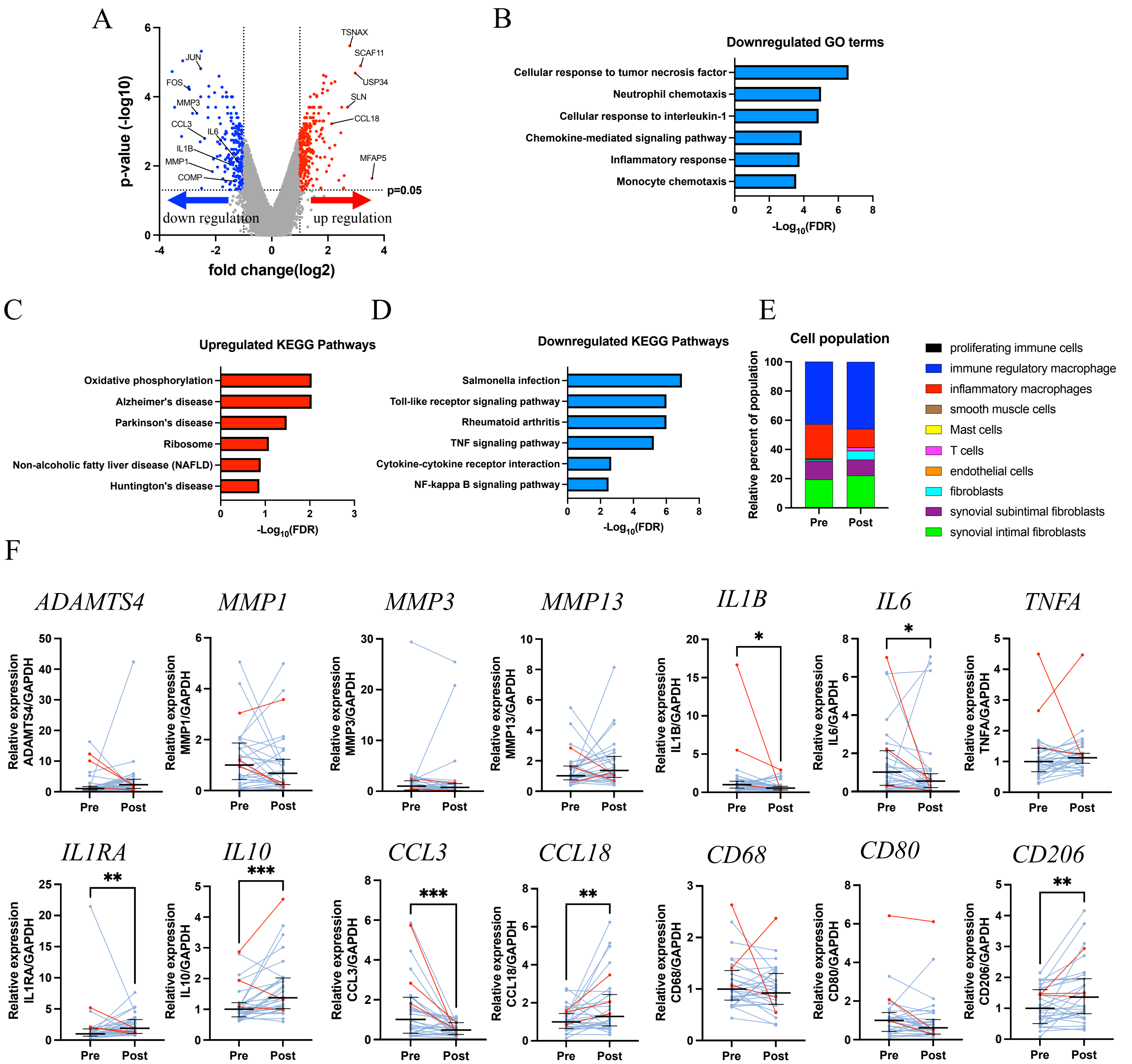

Figure 2

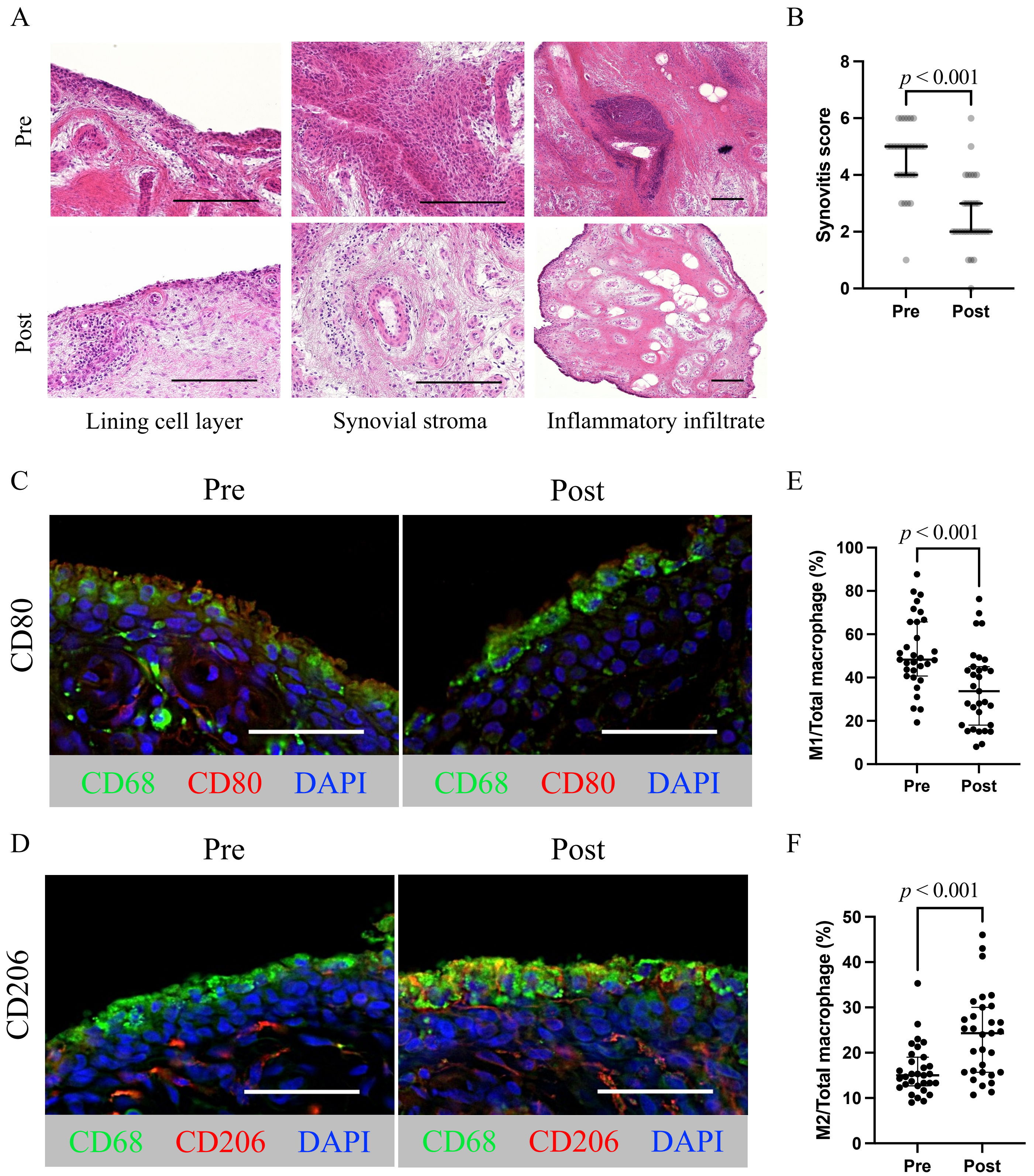

Figure 3

A

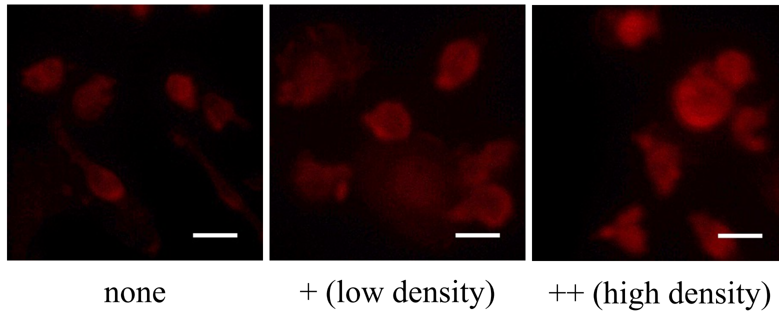

B

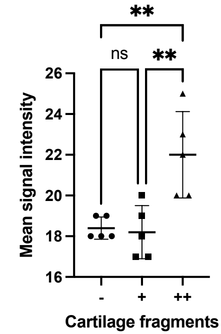

C.

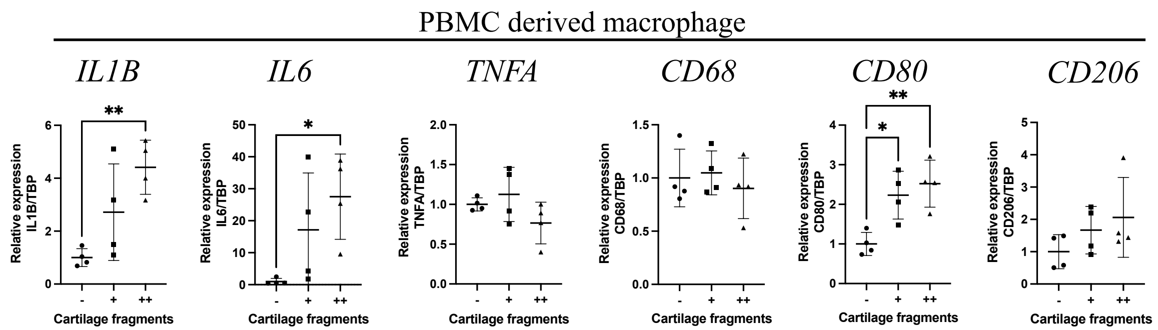

D.

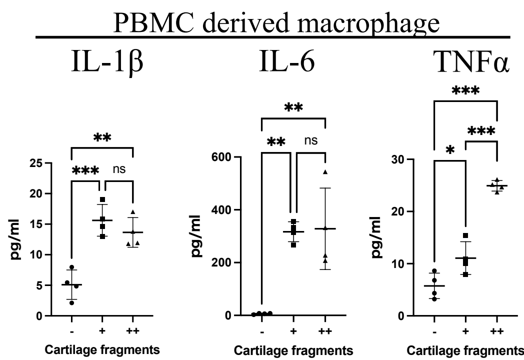

E

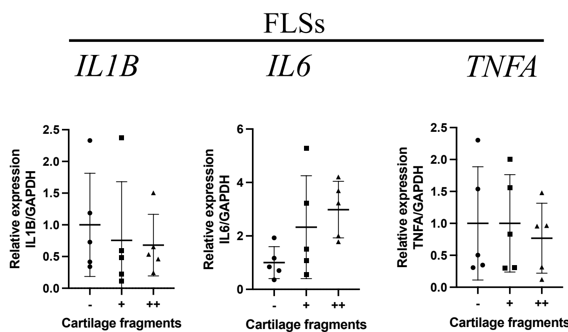

F

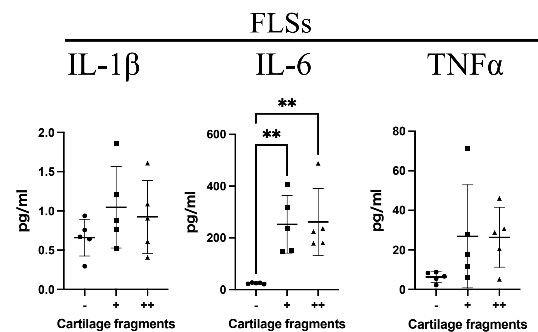

Figure 4

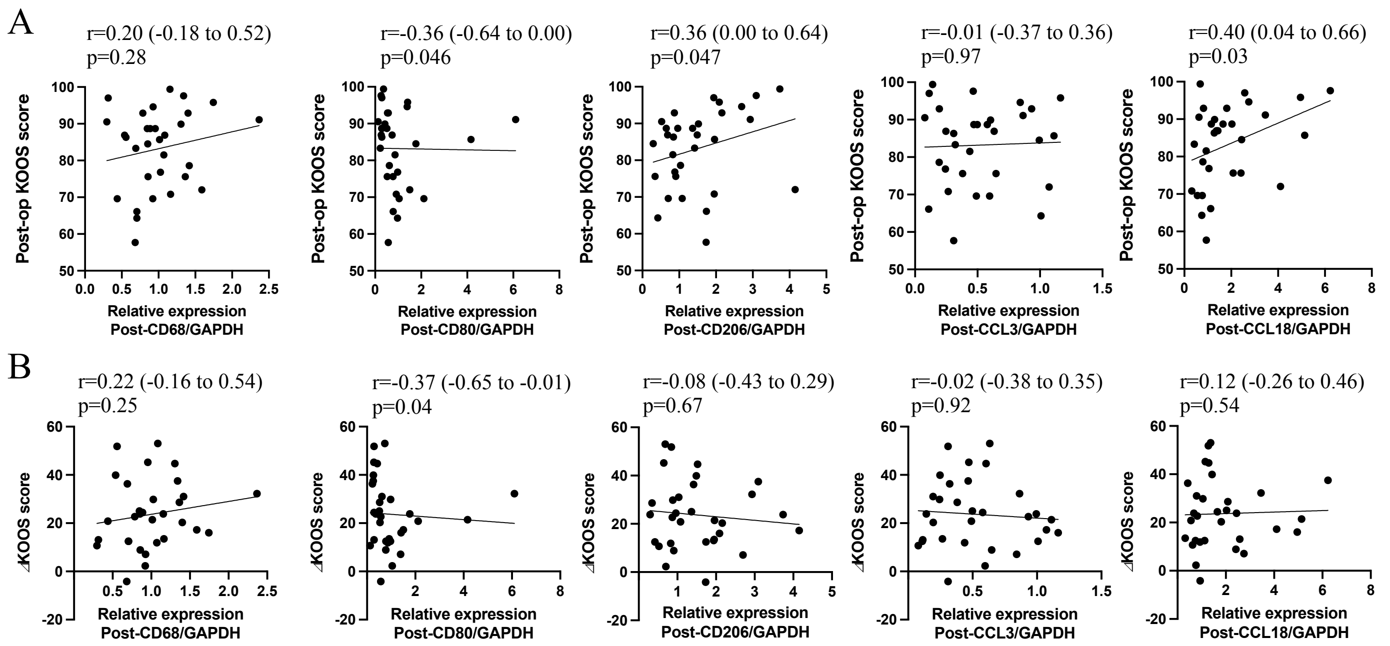

Figure 5